

High-resolution microscopy without high-numerical-aperture lenses: standing-wave scanning fluorescence microscopy

Stanley S. Hong, Michael S. Mermelstein, Berthold K. P. Horn, and

Dennis M. Freeman

December 11, 2004

Abstract

We propose and demonstrate a new type of far-field fluorescence microscope capable of sub- λ resolution without high numerical aperture (NA) lenses. In the new standing-wave scanning fluorescence microscope, focused illumination is generated by the interference of a large number of planar wavefronts. Scanning confocal detection eliminates the need for modulation of wavefront phases during image formation. We measure a point-spread function less than 290 nm in lateral diameter ($\lambda_{\text{exc}} = 488$ nm) with a working distance of 22 mm using 15 illumination wavefronts and a 0.25-NA objective lens.

In 1873 Ernst Abbe discovered that the resolving power of an optical microscope is related by diffraction to the numerical aperture (NA) of the objective lens [1]. The discovery established that conventional high-resolution microscopy requires high-NA lenses. Unfortunately, the difficulties associated with designing and constructing high-NA lenses give rise to many practical limitations in optical microscopy. For example, the working distance of a typical 1.4-NA oil-immersion objective (i.e., a high-NA lens) is only several hundred micrometers, severely limiting both the variety of specimens

that can be imaged and physical access for probes and other instruments. Also, high-NA lenses are not amenable to mass-fabrication or microfabrication, rendering optical microscopes too large and expensive for many applications in education and research.

Recent work in fluorescence microscopy using standing-wave (SW) illumination has begun to suggest that high-resolution optical microscopy may be feasible *without* high-NA lenses. In 1993, it was demonstrated that the axial resolution of a fluorescence microscope could be improved by illuminating specimens with an interference pattern generated by two counterpropagating laser beams (i.e., SW illumination) [2, 3]. Since then, the physical principle has been put on solid theoretical footing and demonstrated experimentally in numerous configurations [4, 5, 6, 7, 8, 9, 10, 11, 12, 13, 14]. The optical-transfer-function (OTF) support of two SW fluorescence microscopes is shown in Fig. 1. With a sufficient number of wavefronts, contiguous coverage of spatial frequency up to the diffraction limit can be achieved using a low-NA lens. Although such use of large numbers of wavefronts has been proposed [4, 10, 14], a SW fluorescence microscope with more than two pairs of wavefronts has not been demonstrated experimentally due largely to the technical complexities of controlling the large number of wavefront phases. In this letter, we propose a new type of fluorescence microscope that combines SW illumination with scanning confocal detection to enable the use of large numbers of wavefronts. We demonstrate a standing wave scanning fluorescence microscope (SWSFM) with 15 wavefronts and a 0.25-NA objective lens that achieves a measured point spread function less than 290 nm in lateral diameter with a working distance of 22 mm.

Figure 2 shows a schematic diagram of the SWSFM. The microscope can be de-

scribed as a Type 2 scanning fluorescence microscope where the illumination objective lens has been replaced by SW illumination [15]. Note that in contrast to previously reported widefield microscopes that utilize SW illumination, the SWSFM does not require modulation of wavefront phases during image formation. Image formation can be described by a point-spread function (PSF) that is the product of an excitation PSF and a detection PSF: $h(\mathbf{r}) = h_{\text{exc}}(\mathbf{r})h_{\text{det}}(\mathbf{r})$, where \mathbf{r} is a three-dimensional (3-D) position vector. The standing wave generated by N electromagnetic plane waves of identical temporal frequency can be written $\mathbf{E}(\mathbf{r}) = \sum_{n=1}^N \mathbf{E}_n \exp(j\mathbf{k}_n \cdot \mathbf{r})$, where \mathbf{E}_n and \mathbf{k}_n denote the complex electric-field vector and wave vector of the n th plane wave, respectively. Assuming that fluorescence excitation is proportional to the time-averaged electric energy density, the excitation PSF can be written

$$h_{\text{exc}}(\mathbf{r}) = \langle \|\mathbf{E}(\mathbf{r}, t)\|^2 \rangle \quad (1)$$

$$= \frac{1}{2} \mathbf{E}(\mathbf{r}) \cdot \mathbf{E}^*(\mathbf{r}) \quad (2)$$

$$= \sum_{n=1}^N \frac{\|\mathbf{E}_n\|^2}{2} + \sum_{m=1}^{N-1} \sum_{n=m+1}^N |\mathbf{E}_m| \cdot |\mathbf{E}_n| \cos[(\mathbf{k}_m - \mathbf{k}_n) \cdot \mathbf{r} + (\angle \mathbf{E}_m - \angle \mathbf{E}_n)] \quad (3)$$

where $\langle \cdot \rangle$ denotes time-averaging, $\|\cdot\|$ denotes length, $*$ denotes complex conjugate, $|\cdot|$ denotes complex modulus, and \angle denotes complex phase. The corresponding excitation OTF can be written

$$H_{\text{exc}}(\mathbf{f}) = \mathcal{F} \left\{ \frac{1}{2} \mathbf{E}(\mathbf{r}) \cdot \mathbf{E}^*(\mathbf{r}) \right\} \quad (4)$$

$$= \frac{1}{2} \mathcal{F} \{ \mathbf{E}(\mathbf{r}) \} \star \mathcal{F} \{ \mathbf{E}(\mathbf{r}) \} \quad (5)$$

$$= \frac{1}{2} \left\{ \left[\sum_{n=1}^N \mathbf{E}_n \delta(\mathbf{f} - \mathbf{k}_n) \right] \star \left[\sum_{n=1}^N \mathbf{E}_n \delta(\mathbf{f} - \mathbf{k}_n) \right] \right\}, \quad (6)$$

where \mathbf{f} is a 3-D spatial-frequency vector, \mathcal{F} denotes the 3-D Fourier transform, \star denotes 3-D cross-correlation, and $\delta(\mathbf{f})$ is the unit impulse. A low-NA objective lens can be satisfactorily represented in two dimensions as an incoherent imaging system with a circular pupil function [16]; the detection PSF can correspondingly be written $h_{\text{det}}(\mathbf{r}) = [J_1(2\pi wr)/(\pi wr)]^2$, where J_1 is the first-order Bessel function of the first kind, $w = NA/\lambda_{\text{em}}$, and $r = \|\mathbf{r} \cdot (\hat{\mathbf{x}} + \hat{\mathbf{y}})\|$.

To demonstrate the SWSFM concept, a SWSFM with 15 wavefronts and a 0.25-NA objective lens was constructed. A SW-illumination apparatus generates 15 linearly-polarized laser beams ($\lambda = 488$ nm) split from a single-frequency argon ion laser (Coherent, Santa Clara, California). The 15 beams are directed by an assembly of mirrors into a converging circular cone with a half-angle of 72 degrees, corresponding to an excitation NA of 0.95. One mirror in each beam path is mounted on a piezoelectric actuator, allowing the phase of each beam to be modulated independently. The beams are transverse-magnetic polarized with respect to the x - y image plane, resulting in radially-polarized illumination. The working distance of the SW-illumination apparatus (i.e., the axial distance between the apparatus and the sample) is 22 mm. The SW-illumination apparatus is described in more detail elsewhere [17]. The sample is mounted on a two-axis closed-loop piezoelectric scanning stage (Melles Griot, Carlsbad, California). Fluoresced light is collected by an $10\times / 0.25$ NA objective lens and focused onto a $15\text{-}\mu\text{m}$ -diameter pinhole. Excitation light is rejected by a 3-mm-thick

OG-515 glass filter (Schott, Elmsford, New York), and fluoresced light is measured by a photon-counting photomultiplier tube (Hamamatsu Photonics, Bridgewater, New Jersey).

Figures 3 and 4 show the calculated 2-D PSF and OTF, respectively, of the constructed 15-wavefront SWSFM. The amplitudes and phases of the 15 plane waves are equal at the center of the PSF (i.e., all $\|\mathbf{E}_n\|$ have the same complex value). Note that both the diameter of the PSF and the highest spatial frequency in the OTF support are determined primarily by the SW excitation and not the low-NA lens detection. With a given SW-illumination apparatus, contiguity requirements of the OTF establish a lower bound on the NA of the objective lens. The large “height” of singularity at the origin of the excitation OTF can be attributed to the orientations of the wave vectors \mathbf{k}_n , which were specifically designed to affect only lateral resolution. Consequently, the excitation PSF of the constructed microscope is a propagation-invariant or “nondiffracting” field [18]. In the limit that the number of wavefronts generating propagation-invariant SW illumination approaches infinity, the excitation PSF is in fact a radially-polarized vector Bessel beam [19], and the area under the singularity is unbounded since Bessel beams are not absolutely integrable.

Figure 5 shows the lateral response of the constructed 15-wavefront SWSFM to an isolated 200-nm-diameter fluorescent polystyrene bead (Molecular Probes, Eugene, Oregon). The bead was deposited on a glass coverslip and imaged in air. The SW illumination was directly incident on the bead while the fluoresced light was imaged through the coverslip. Lens aberrations introduced by the coverslip are negligible at 0.25 NA. The reflection of the SW illumination off the air-to-glass interface of the

coverslip was expected to widen the diameter of the lateral response by less than 6%. The phases of the 15 illumination wavefronts were aligned prior to imaging by maximizing the light fluoresced by a different 200-nm-diameter bead (not shown). Confocal alignment between the SW illumination and objective lens was achieved by positioning the bead at the center of the detection PSF during phase alignment. The algorithm for adjusting the individual wavefront phases is guaranteed to converge monotonically and was tested using the constructed microscope with both fluoresced and coherently scattered light [20].

Figure 6 compares the resolving power of the constructed microscope using conventional widefield illumination and using SW illumination. The sample of 500-nm-diameter fluorescent polystyrene beads (Molecular Probes, Eugene, Oregon) was prepared and imaged using the same techniques as in Fig. 5. Without SW illumination, the constructed microscope functions as a conventional Type 1 scanning fluorescence microscope, and resolving power is derived solely from the 0.25-NA objective lens.

The resolution of the SWSFM is limited ultimately by diffraction and thus cannot significantly exceed that of the 4Pi confocal fluorescence microscope [21]. As demonstrated with the 4Pi confocal fluorescence microscope, the resolution of the SWSFM could in principle be improved by utilization of nonlinear fluorescence excitation [22, 23] or by cascade with image restoration [24, 25]. However, we expect that the SWSFM will be most valuable as a means for circumventing the requirement and subsequent limitations of high-NA lenses in high-resolution optical microscopy. For example, the essential components of a SWSFM may be amenable to microfabrication; the subsequent reduction in both size and cost compared to conventional

high-resolution microscopes may make implantable microscopes practical for chronic in-vivo imaging of tissue with sub-cellular resolution.

In summary, a new type of microscope that combines SW illumination and scanning confocal detection has been proposed. The concept has been verified experimentally by demonstrating a microscope capable of sub- λ resolution using 15-wavefront SW illumination and a 0.25-NA objective lens. The SWSFM represents a new path to high-resolution optical microscopy without high-NA lenses.

The authors wish to acknowledge H. I. Smith, P. T. C. So, C. C. Abnet, J. F. Deck, J. Fini, and A. J. Aranyosi for their contributions. This work was supported by the Defense Advanced Research Projects Agency (DARPA) under grant N66001-02-1-8915.

References

- [1] E. Abbe, “Beitrage zur Theorie des Mikroskops und der mikroskopischen Wahrnehmung,” *Arch. Mikrosk. Anat.* **9**, 413 (1873).
- [2] F. Lanni, *Applications of Fluorescence in the Biomedical Sciences*, (Liss, New York, 1986).
- [3] B. Bailey, D. L. Farkas, D. L. Taylor, and F. Lanni, “Enhancement of axial resolution in fluorescence microscopy by standing-wave excitation,” *Nature* **366**, 44 (1993).
- [4] F. Lanni, B. Bailey, D. L. Farkas, and D. L. Taylor, “Excitation field synthesis as a means for obtaining enhanced axial resolution in fluorescence microscopy,” *Bioimaging* **1**, 187 (1994).
- [5] M. A. A. Neil, R. Juškaitis, and T. Wilson, “Method of obtaining optical sectioning by using structured light in a conventional microscope,” *Opt. Lett.* **22**, 1905 (1997).
- [6] R. Heintzmann and C. Cremer, “Laterally modulated excitation microscopy: improvement of resolution using a diffraction grating,” *Proc. SPIE* **3568**, 185 (1998).
- [7] G. E. Cragg and P. T. C. So, “Lateral resolution enhancement with standing evanescent waves,” *Opt. Lett.* **25**, 46 (2000).
- [8] M. G. L. Gustafsson, “Surpassing the lateral resolution limit by a factor of two using structured illumination microscopy,” *Journal of Microscopy* **198**, 82 (2000).

- [9] J. T. Frohn, H. F. Knapp, and A. Stemmer, “True optical resolution beyond the Rayleigh limit achieved by standing wave illumination,” *PNAS* **97**, 7232 (2000).
- [10] J. T. Frohn, H. F. Knapp, and A. Stemmer, “Three-dimensional resolution enhancement in fluorescence microscopy by harmonic excitation,” *Opt. Lett.* **26**, 828 (2001).
- [11] M. Nagorni and S. W. Hell, “Coherent use of opposing lenses for axial resolution increase in fluorescence microscopy. I. Comparative study of concepts,” *J. Opt. Soc. Am. A* **18**, 36 (2001).
- [12] P. T. C. So, H.-S. Kwon, and C. Y. Dong, “Resolution enhancement in standing-wave total internal reflection microscopy: a point-spread engineering approach,” *J. Opt. Soc. Am. A* **18**, 2833 (2001).
- [13] R. Heintzmann, T. M. Jovin, and C. Cremer, “Saturated patterned excitation microscopy—a concept for optical resolution improvement,” *J. Opt. Soc. Am. A* **19**, 1599 (2002).
- [14] J. Ryu, B. K. P. Horn, M. S. Mermelstein, S. S. Hong, and D. M. Freeman, “Application of structured illumination in nano-scale vision,” presented at the IEEE Workshop on Computer Vision for the Nano-Scale, Madison, Wisconsin, 16–22 June 2003.
- [15] C. J. R. Sheppard and A. Choudhury, “Image formation in the scanning microscope,” *Optica Acta* **24**, 1051 (1977).

- [16] T. Wilson and C. J. R. Sheppard, *Theory and Practice of Optical Scanning Microscopy* (Academic, London, 1984).
- [17] S. S. Hong, M. S. Mermelstein, B. K. P. Horn, and D. M. Freeman are preparing a manuscript to be called “Lensless focusing of light using direct angular spectrum synthesis.”
- [18] J. Durnin, “Exact solutions for nondiffracting beams. I. The scalar theory,” *J. Opt. Soc. Am. A* **4**, 651 (1987).
- [19] Z. Bouchal and Marek Olivík, “Non-diffractive vector Bessel beams,” *Journal of Modern Optics* **42**, 1555 (1995).
- [20] S. S. Hong and D. M. Freeman are preparing a manuscript to be called “Phase alignment for standing-wave illumination microscopy by iterative maximization of point intensity.”
- [21] S. W. Hell and E. H. K. Stelzer, “Properties of a 4Pi confocal fluorescence microscopy,” *J. Opt. Soc. Am. A* **9**, 2159 (1992).
- [22] S. W. Hell, “Fundamental improvement of resolution with 4Pi-confocal fluorescence microscopy using two-photon excitation” *Opt. Commun* **93**, 277 (1992).
- [23] M. Dyba and S. W. Hell, “Focal Spots of Size $\lambda/23$ Open Up Far-Field Fluorescence Microscopy at 33 nm Axial Resolution,” *Phys. Rev. Lett.* **88**, 163901 (2002).

- [24] S. W. Hell, M. Schrader, and H. T. M. van der Voort, “Far-field fluorescence microscopy with three-dimensional resolution in the 100-nm range,” *J. Microsc.* **187**, 1 (1997).
- [25] M. Nagorni and S. W. Hell, “4Pi-Confocal Microscopy Provides Three-Dimensional Images of the Microtubule Network with 100- to 150-nm Resolution,” *J. Struct. Biol.* **123**, 236 (1998).

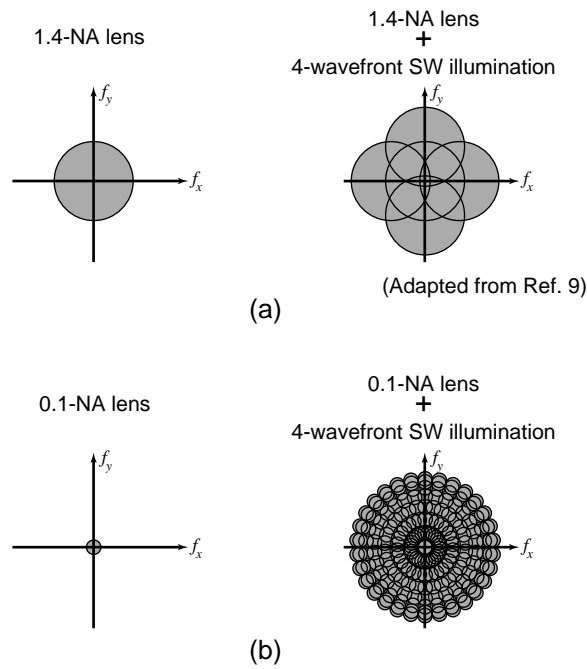


Figure 1

Figure 1: Effect of SW illumination on OTF support. (a) The left illustration shows the OTF support of a high-NA objective lens using conventional widefield illumination. The right shows the OTF support of the same lens using four illumination wavefronts. (b) Analogous illustrations with a low-NA lens and using a large number of illumination wavefronts.

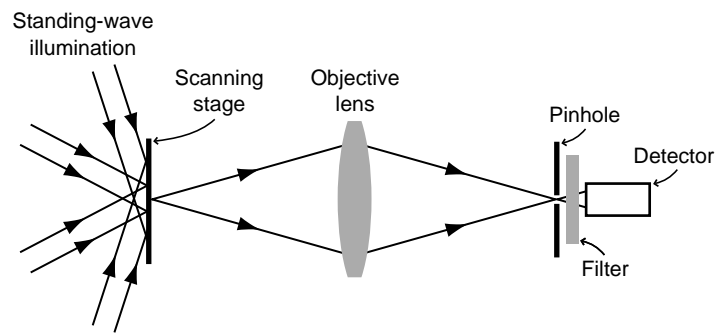


Figure 2

Figure 2: Schematic diagram of the SWSFM.

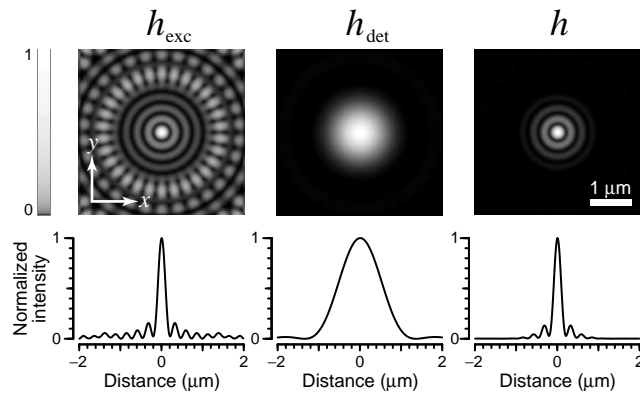


Figure 3

Figure 3: Calculated 2-D intensity PSF of the constructed 15-wavefront SWSFM. The images show the excitation, detection, and overall PSF in the x - y plane. The plots show the intensity through the center of each PSF. Note the logarithmic grayscale used to show low-intensity features. The FWHM diameter of the overall PSF is 200 nm.

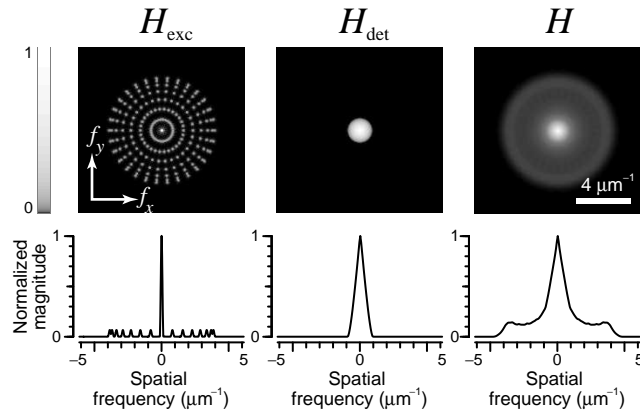


Figure 4

Figure 4: Calculated 2-D OTFs of the constructed 15-wavefront SWSFM. The images show the excitation, detection, and overall OTF in the f_x - f_y plane. The plots show the magnitude through the center of each OTF. Note the logarithmic grayscale used to show low-intensity features. The “spikes” in the excitation OTF represent singularities.

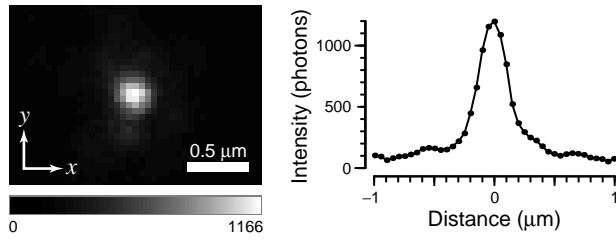


Figure 5

Figure 5: Measured 2-D intensity PSF of the constructed 15-wavefront SWSFM. The image shows an isolated 200-nm-diameter bead imaged with the constructed microscope. The plot shows the center row of pixels in the image. The step size is 50 nm, and the FWHM diameter of the peak is 290 nm.

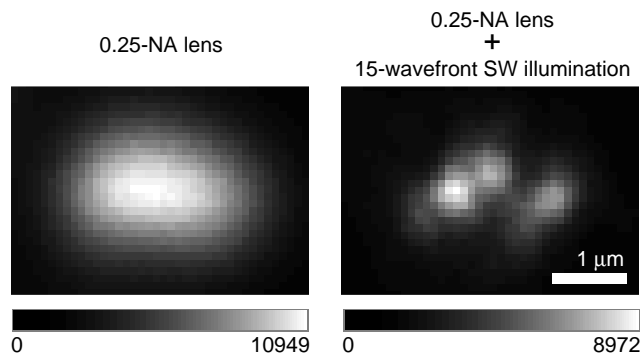


Figure 6

Figure 6: Effect of SW illumination on image resolution. The images show the same cluster of three 500-nm-diameter beads imaged with the constructed 15-wavefront SWSFM. In the left image, SW illumination was temporarily disabled and replaced with conventional widefield illumination. In the right image, SW illumination was restored. The step size is 100 nm.